ARTICLE IN PRESS

Materials Today: Proceedings xxx (xxxx) xxx

Contents lists available at ScienceDirect

Materials Today: Proceedings

journal homepage: www.elsevier.com/locate/matpr

# Magnetic field assisted 3D printing of short carbon fibre-reinforced polymer composites

Celia Pearson [a], Sara Hawi [b], Cristian Lira [c], Saurav Goel [d,e,f], Hamed Yazdani Nezhad [a,*]

[a] Aeronautics and Aerospace Research Centre, Department of Mechanical Engineering and Aeronautics, City, University of London, London, UK
[b] School of Aerospace, Transport and Manufacturing, Cranfield University, UK
[c] Engineering Development, National Composites Centre, Bristol, UK
[d] School of Engineering, London South Bank University, London, UKd School of Engineering, London South Bank University, London SE10 AA, UK
[e] University of Petroleum and Energy Studies, Dehradun 248007, India
[f] Indian Institute of Technology Guwahati, Guwahati 781039, India

ARTICLE INFO

*Article history:*
Available online xxxx

*Keywords:*
Polymer composites
Carbon fibre
3D printing
Magnetic field
Fibre orientation
Short fibres
FDM

ABSTRACT

This paper investigates and discusses the outcomes from an ongoing feasibility research being conducted at Advanced Composites Research Focused Group on 3D printing polymers and carbon composites subjected to localised magnetic field force lines. Magnetic equipped composite processes are starting to become an important new development for structural applications. Specific to this paper, in-situ alignment of short carbon fibres (~1 mm length) in thermoplastic polymer filaments (Onyx FR, a Nylon base with micro carbon-fibres with a flame retardant additive supplied by Markforged) during a fused deposition modelling (FDM) based 3D printing (MakerBot Replicator 2). An experiment took place in which samples of PLA and onyx were printed, both with and without a magnetic field present. This was done to see what effects, if any, the magnetic field had on the flow orientation of these materials when printed. The results from using a high-resolution optical microscopy and scanning electron microscopy showed that while carbon fibres within the Onyx had aligned in response to the magnetic field, the PLA samples were visibly unchanged by the magnetic field. The observations have been partially supported by theoretical calculations utilizing Multiphysics constitutive equations.


## 1. Introduction

3D printing is an additive manufacturing (AM) technique and is used to fabricate various structures using CAD. It works by placing a material on a printing bed and adding layer-upon-layer to manufacture a component [1,2]. In 1984, Charles Hull invented a technique called stereolithography, this is the first recorded method of 3D printing. Stereolithography is the 3D printing of objects using solid layers of ultraviolet light sensitive resin. A few years after this, in 1988, Scott Crump invented the fused deposition modelling (FDM) based 3D printing technique, which is still the most common method of 3D printing used today [3]. 3D printing has been a main topic of scientific interest over the last three decades. It offers many advantages over traditional manufacturing including a reduction in time, material and cost wastage, as well as an increased range of complex structures and design freedom [4,5]. The most prominent of these advantages is the reduction of the need for post processing requirements [4]. For these reasons, 3D printing has been revolutionary in a broad range of manufacturing related industries [6]. AM is becoming increasingly used in areas such as design, art, biomedicine, aerospace, automotive parts and energy [7].

There are different variations of 3D printing techniques, and each is useful for simplifying design manufacture in its own way [7]. There are seven main processes for 3D printing polymeric materials: Material Extrusion, Binder Jet- ting, Sheet Lamination, Material Jetting, Vat Photo-polymerisation, Direction Energy Deposition and Powder Bed Fusion. Out of these procedures, Material Extrusion, Material Jetting, Vat Photo-polymerisation and Powder Bed Fusion are the techniques most commonly used in the 3D printing of magnetoactive composites.

* Corresponding author.
*E-mail address:* hamed.yazdani@city.ac.uk (H. Yazdani Nezhad).

https://doi.org/10.1016/j.matpr.2022.04.597
2214-7853/

Please cite this article as: C. Pearson, S. Hawi, C. Lira et al., Magnetic field assisted 3D printing of short carbon fibre-reinforced polymer composites, Materials Today: Proceedings, https://doi.org/10.1016/j.matpr.2022.04.597

In this project two types of material were used as the filament: PLA, which is a polymer, and Onyx carbon fibre-reinforced composite. FDM is a type of Material Extrusion technique [8], and is the method used mainly for thermoplastic polymers and polymeric composites, such as low temperature process PLA and high temperature Poly-ether-ether-ketone, offering higher fracture toughness and damage tolerance compared to their thermoset based rivals [9]. Due to the extensive research into the uses and benefits of FDM and the simplicity and low cost of this method, it was the technique of choice this project. In simple terms, FDM is a material extrusion technique that deposits a wire of polymer filament through a heated nozzle. The molten filament is then deposited precisely in a unique pattern on the printing bed to build each layer of the component being printed. This depositing mechanism makes FDM particularly useful for multi-material composite printing [7] or for multifunctional material development such as those for self-sensing, toughening and property tailoring [10–12]. The layers are added one after the other until the final component is produced. A diagram of a front view of the FDM process examined in this research is illustrated in Fig. 1.

Until very recently, polymers were generally considered to be unaffected by magnetic fields. However, it is now known that they are weakly magnetized because they are diamagnetic materials, and therefore do respond to magnetic fields [13]. The main ways in which polymer composites are magnetised are by melting the polymers or placing them in a liquid suspension to break up the cross-links, so that when the magnetic field is applied, the fibres within the polymer composites realign. There are other methods in which various industries have tried to assemble the fibres within materials. These include mechanisms such as shear, electrical and ultrasonic alignment. However, magnetic alignment, has gained the most attention and has been proven to be the top choice to achieve alignment for a few reasons. Firstly, magnetic forces are contactless, so will not produce any chemical alteration within the material, but still allow the orientation of anisotropic particles. Secondly, permanent magnets and electromagnets are easy to come by and still produce strong enough fields for reorientation. Thirdly, the magnetic fields can be homogeneous, inhomogeneous, rotating or oscillating, and each allows a variety of responses and therefore a variety of structures produced. Fourthly, the response depends on the magnetism of the material, which depends on the susceptibility (e.g. whether the material is ferromagnetic or diamagnetic etc). Lastly, magnetic fields are not sensitive to surface changes or pH, unlike electric fields [14,15].

The magnetic alignment of CFs in suspension has been researched since 1972, and their incorporation into polymer composites has been described. In 2010, a report was published in which composites with CFs were aligned using a Neodymium magnet, which produced a field that oriented the CFs at different angles. It was from this that scientists found the material could deform when subjected to a homogeneous magnetic field. CFs possess a large diamagnetic anisotropy, which can produce a strong torque under an applied magnetic field. This torque produces a curvature of the composite. An experiment in 2016 took place where the fibres were aligned parallel to the applied magnetic field direction produced by four Neodymium magnets as opposed to just one, in order to further enhance the properties. These fibre reinforced polymer composites are widely used in many industries including automotive, aerospace, marine and construction, due to their unique properties including corrosion resistance and high strength and modulus [15,16].

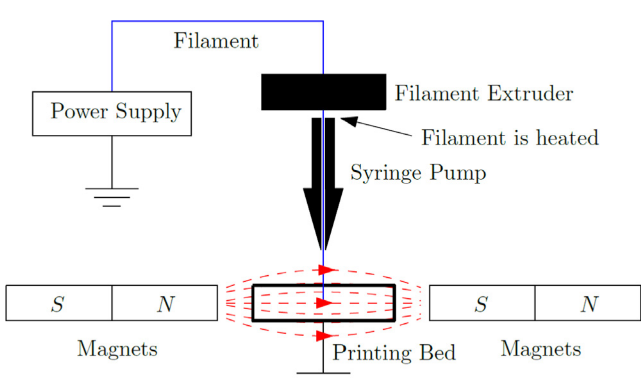


**Fig. 1.** Diagram of the front view of FDM technique with magnets on either side of the printing bed, where the red dashed line represents the magnetic field going from the north to south pole. (For interpretation of the references to colour in this figure legend, the reader is referred to the web version of this article.)

## 2. Theoretical background

This project is the beginning state of a much longer vision. The aim for this overall vision is to 3D develop complex magnetic composites for space applications. However, the aim of this project is to see how polymers and carbon composites react to a strong magnetic field when they are being processed and are not yet fully consolidated. The expectation is that the fibres within the materials realign when subject to the magnetic field, which should be visible in optical microscopy. To do so, the setup and design of the samples were varied to see how the magnetic field changes the alignment of the fibres inside the 3D printed cuboid design (magneto-assisted printing). This is very important for engineering applications due to the potential to strengthen the material being printed and alter other mechanical properties. That being stated, it will be very difficult to magnetize a polymer as they are tightly packed together. Thermoplastic polymers are formed by consolidating several chains together to create strong covalent bonds. As a result of this type of formation, the substance formed is rigid and hard [17].

Liquid crystalline polymers are easily able to respond to an applied magnetic field and undergo magnetic alignment. In the past it was considered that solid crystalline polymers were unable to experience alignment because they lack the liquid crystalline phase required to respond to the applied field. Using this logic, a molten polymer or polymer composite should be able to respond to an external magnetic field as the level of consolidation within the polymer is reduced. This is where the 3D printing comes in. The polymer filament is made molten in the heated nozzle at the beginning of the printing process, and theoretically this could affect the magnetic alignment of the printed part. It has also been found in literature that many crystalline polymers such as poly (ethylene-2,6-naphthalate) and isotactic polystyrene have been able to align in the suitable conditions [18,19].

The phase transitions in polymer systems are not completed instantly, and some of the crystal structure may not have fully melted even after the temperature has passed the melting point, $T_m$. This phenomenon is known as the “memory effect”. If the magnetic field is applied before the “memory effect” has disappeared, then the viscosity is low and there is still some structure, so there is a high chance of magnetic alignment. The $T_m$ of PLA is 115 °C–150 °C [20], and for Onyx is 145 °C [21], and the temperature of the extruder is heated to is 230 °C and 280 °C respectively. If the maximum temperature is much higher than the melting point of the material, it was found that magnetic alignment would not occur, this suggests that the “memory effect” has a big effect on the alignment [19].

For diamagnetic materials, the magnetic energy is usually tiny, and therefore difficult to distinguish from other energies, such as electric and thermal. However, despite its size, it is still effective.

The diamagnetic properties of a material are directly related to the magnetic susceptibility. The magnetic susceptibility indicates whether a material is attracted to or repelled by a magnetic field. The magnetic anisotropy of a molecule arises from the magnetic anisotropy of its chemical bonds. As discussed in the introduction, if the material has an anisotropy in diamagnetism, a magnetic torque acts on it, resulting in rotation. The origin of magnetic anisotropy is traced back to chemical bonds.

The magnetic effects on diamagnetic materials have very recently been used for the processing of polymeric materials. This is partially due to the development of superconducting technology, with the ability to produce very large magnetic fields. Very large magnetic fields make it possible to visualise the magnetic effects on diamagnetic materials. The origin of diamagnetism is the induced magnetization caused by the induced motion of electrons under the applied magnetic field, where magnitude of the magnetization induced is proportional to the applied field strength. This induced magnetization causes a chemical shift, which can be detected by analysis in Raman spectroscopy [19,22]. In order to predict whether the diamagnetic alignment may occur, the following equations can be used: The magnetisation, $M$ is induced by an applied magnetic field, $H$:

$$M = \chi H \tag{1}$$

where $\chi$ is the magnetic susceptibility, which indicates whether a material is attracted to or repelled by a magnetic field. Let $\chi i$ be the component of $\chi$ in the direction of the particle axis and let $\chi\perp$ be the component perpendicular to the axis. Finally, let $\chi a = \chi i - \chi\perp$. The interaction of the magnetisation with the applied magnetic field gives rise to a magnetic energy, $E_{mag}$:

$$E_{mag} = -0.5V\left(\chi_{\perp}\mu_0^{-1}B^2 + \chi_a\mu_0^{-1}B^2\cos^2\eta\right) \tag{2}$$

where $V$ is the volume of the particle, $\mu 0$ is the magnetic permeability of the vacuum, and $\eta$ is the angle between the magnetic flux density, $B$ and the particle axis. One of the Maxwell's approximation equations is used:

$$B = \mu_0 H. \tag{3}$$

The second term in the magnetic energy equation is orientation-dependent, as this is the source of magnetic alignment. A macroscopic alignment is possible when this second term exceeds the thermal energy, $k_BT$:

$$V > 2kBT\mu_0|\chi_a|B^2. \tag{4}$$

From here, it is estimated that to ensure that alignment takes place, the mini- mum critical volume is needed. The torque, $\boldsymbol{N}$, acting on the particle is:

$$\boldsymbol{N} = V\chi_a\mu_0^{-1}B^2 sin\eta cos\eta\boldsymbol{\omega}, \tag{5}$$

where $\boldsymbol{\omega}$ is a unit vector normal to $n$ and $B$. So, for the magnetic alignment to occur, the particle should have anisotropic diamagnetic susceptibility and the size of the particle must be large enough to overcome the thermal energy [19]. To calculate the correlation of the twist in a short carbon fibre's response to the applied magnetic field, the following equation for the twisting angle can be calculated:

$$\psi(s) = (\psi_m/l)s, \tag{6}$$

where $\psi(s)$ is the twisting angle of the beam section, $\psi_m$ is the magnetic free energy density and $s$ is the length of the beam section. In order to calculate the twisting angle, $\psi_m$ must be calculated from the following equation:

$$\psi_m = -(\chi/2)(\boldsymbol{n}.\boldsymbol{B})2 \tag{7}$$

where $\chi$ is first calculated using.

$$\chi = \chi_a v_f/2\mu_0, \tag{8}$$

where $v_f$ is the volume fraction. This $v_f$ was calculated as 16% according to the Onyx specifications [21,23], and $\chi_a$ was found to be $28 \times 10^6$ [24]. Therefore:

$$\chi = (28\times10^{-6}\times0.16)/(2\times1.26\times10^{-6}) = 1.78, \tag{9}$$

and, using Equation (3) to calculate the magnetic flux density, where $H$ is the field of the N52 magnet (utilized in this research) at 1.48 T [20]:

$$B = 1.26\times10^{-6}\times1.47 = 1.85\times10^{-6}T \tag{10}$$

From here we can calculate $\psi_m$ as:

$$\psi_m = -\left(\frac{17.8}{2}\right)\left(1\times1.85\times10^{-6}\right)^2 = -3.046\times10^{-11} joule/cm. \tag{11}$$

Therefore, the twisting angle is:

$$\psi(s) = (-3.046\times10^{-11}/1000\times10^{-6})5\times10^{-4} = -7.62\times10^{-11} radians \tag{12}$$

where the length of the fibre is 1000 μm, and s is half of this. It makes sense that the fiber moves such a tiny amount due to the presence of one N52 magnet [25]. The number of magnets used have been increased to 10 and 20 to increase the effect on the twisting angle. It is noteworthy that the theoretical calculations provided herein does not address the collective effect arising from numerous short fibres responding within a semi-liquid medium (polymer), and the uncertainties associated with our experimental setup (e.g. carbon fibre type and its magnetization, magnetic field arrangements, spacing, temperature effect on the magnetic field's strength, etc.) are not accounted for.

## 3. Experimental approach

Multiple variables were changed in this experiment to see what, if anything, influences the degree of magnetisation of the printed polymers and carbon composites during the 3D printing process. These variables include an alteration of the materials, the printing precision, and the number of rows of the magnets.

The two types of material used were PLA and onyx, for 3D printing using a MakerBot Replicator 2, but it was used anyway. The precision was altered from standard precision and high precision to see if this would make a difference to how magnetized the print would be. In Fig. 2, the difference between the two precisions is seen: standard has a honeycomb arrangement with 0.2 mm holes

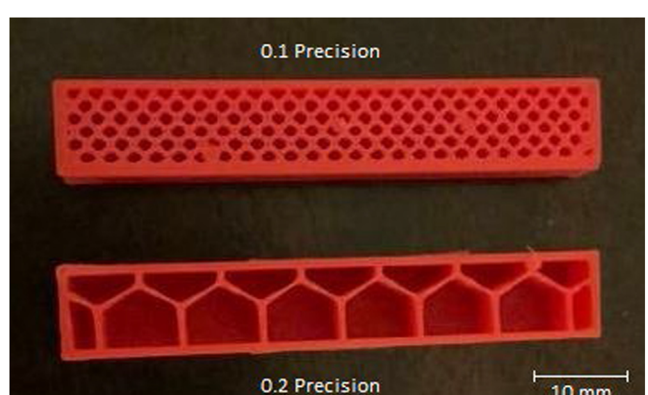


**Fig. 2.** PLA samples of different precisions: The top with high precision 0.1 mm and the bottom with standard precision 0.2 mm.

and high has a more uniform arrangement with 0.1 mm holes. The magnetic field strength type used was the N52 magnet. This is from the critical rare earth metal called neodymium, and each magnets have the dimensions 10 mm × 2 mm. These were set up with five and 10 magnets on either side of the cuboid in rows or one or two magnets, respectively. The aim of trying multiple rows of magnets was to observe how altering the strengths would vary the extent to which the fibres were aligned.

### 3.1. Printing PLA

The printer used was the MakerBot Replicator 2, shown in Fig. 3. PLA has a uniform arrangement of a repeated unit of lactic acid and is a naturally existing polymer. It has a low viscosity and melting point, which makes it suitable for the MakerBot with a temperature limit of 280 °C [7]. To begin with, test samples of the cuboid designs were printed with PLA just to get an understanding of the machine and how it worked, and also to see how it responded to altering various factors, like the precision. After this, it was time to begin printing the samples.

The project involved 3D printing eight cuboids of the dimensions: 10 mm × 60 mm × 12 mm. These cuboids were created in the software Solidworks. Six of these cuboids were printed using the material, PLA, and two were printed using the material onyx. The variations by which these cuboids were printed are:

- 1 row, standard precision, PLA
- 1 row, high precision, PLA
- 2 rows, standard precision, PLA
- 2 rows, high precision, PLA
- No magnetic field, high precision, onyx
- rows, high precision, onyx
- No magnetic field, high precision, PLA
- No magnetic field, standard precision, PLA

The parts printed with the row of magnets had five magnets on either side of the cuboid, as shown in Fig. 4. The magnets were arranged before they were placed inside the machine with five north magnets on the long side of the cuboid, and five south magnets on the other side. The magnetic field lines were expected to look similar to Fig. 1 but in 3D. Tape was placed on top of the printing bed and glue was spread on top of this tape in the area the part was about to be printed. The printer machine was connected to a computer, where the printing is initialized and some parts were set up including the exact location of the part within the printer, the precision of the parts produced, the heat of the bed (110 °C) and the heat of the extruder (230 °C). It was calculated that after 15% of the 12 mm cuboid had been printed, the height would be 2 mm, which is the height of one N52 magnets (as stated above). Therefore after 30%, the cuboid was 4 cm high, which is the height of two of the N52 magnets. At these points, the printer was briefly paused to place the magnets inside in rows of one or two. The reason for this is, the nozzle on the printer must be at exactly the same height as the printing bed, so the nozzle would be obstructed by the magnets if they were placed beside the cuboid. Once the printer reached 80%, the machine was stopped because after this point, the cuboid shape would have been closed up and the printing pattern on the inside not visible.

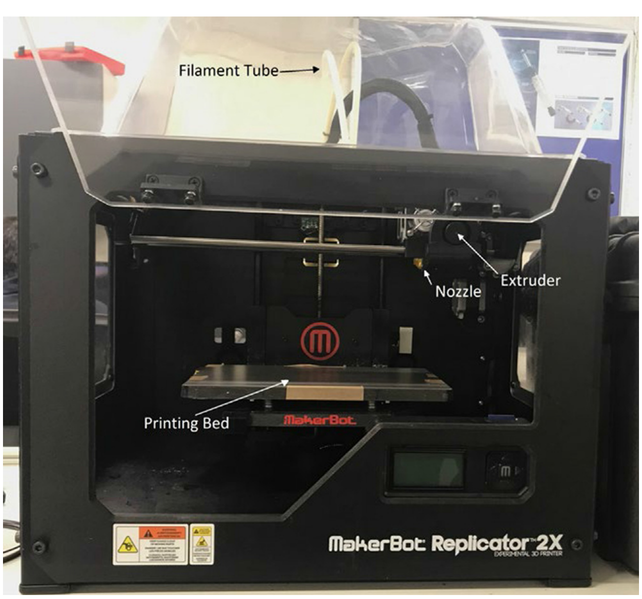


**Fig. 3.** Labelled MakerBot Replicator 2 machine used for 3D printing.

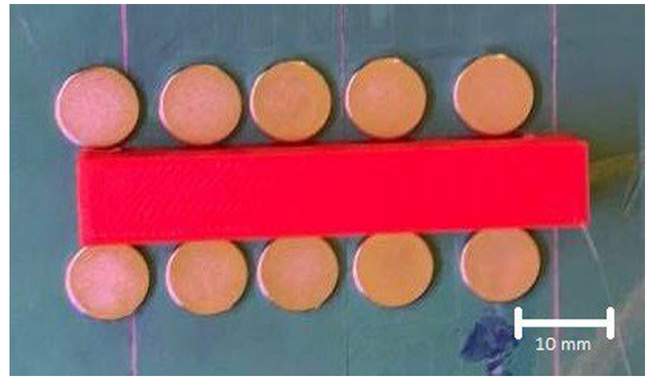


**Fig. 4.** PLA printed cuboid with five N52 magnets of opposite polarity on each side of the cuboid.

### 3.2. Printing onyx

Once all the PLA parts were printed, the next material to use was onyx. Onyx is a micro carbon filled nylon, and it was hypothesized that this would have a different response to the magnetic field than the PLA. The printer was not built to use onyx filament. Because of this, various speeds, temperatures, and printing bed materials were tried. The filament cooling fan speed was changed from 0.5 to 0.1, and the print speeds were also changed, Fig. 5. The level of the printing bed was altered multiple times and therefore so was the nozzle, so that they were the same height. Initially, the onyx would not stick properly to the printing bed for the first attempted variations. Eventually, however, the standard settings for the printing, which were kept the same for each PLA sample, were changed for the onyx to allow the printing to work. Almost all the print speeds were changed, as seen in Fig. 5, and the heat

| Print Speeds [mm/s]: | PLA | Onyx |
|---|---|---|
| Floor Surface Fills | 40 | 40 |
| Infill | 30 | 40 |
| Insets | 50 | 40 |
| Outlines | 90 | 40 |
| Raft | 90 | 40 |
| Raft Base | 90 | 40 |
| Roof Surface Fills | 90 | 40 |
| Sparse Roof Surface Fills | 90 | 40 |

**Fig. 5.** The print speeds settings for PLA and onyx.

of the extruder was increased from 230 °C to 280 °C. This temperature was originally avoided as it exceeded the temperature limit of the machine, and the deteriorating effect on the magnetic field but the onyx would not have been able to stay stuck to the printing bed otherwise. As a result, after the second part printed, the machine's nozzle stopped working, and no more onyx samples could be printed. Magnets are known to be affected by high temperatures, however, they can be re-magnetised over time, though not completely. Therefore, the used magnets were left for at least a few hours before they were used again. Even so, there will be some uncertainty to with the magnetic field strength of the magnet, particularly with onyx as the temperature of the nozzle and extruder was higher than with the PLA [24].

After all the PLA and onyx parts were printed, they were removed using a scalpel and the printer was wiped down with water to remove the glue. The designs were then inspected using a VH-S30F/S30B high magnification optical microscope shown in Fig. 6(a) and investigated in a SEM. In the optical one, the lens was changed from one with a magnification lens of x20 – x200 to one with the range x500 – x5000, called the High-resolution zoom lens, which was the highest magnification available. Each part was examined and around ten photos for each sample were taken, five with the magnification x500 and five with x5000. Various parts of the cuboids and the printing inside were inspected, including the edges, the tilted lines, the straight lines, and the intersections. The microscope was connected to the digital microscope VHX machine pictured in Fig. 6(b).

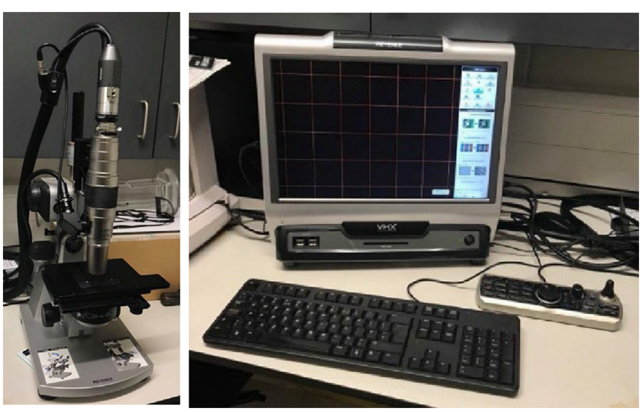

**Fig. 6.** High magnification VHX series digital optical microscopy.

## 4. Results and discussion

From Fig. 7, it is seen that the direction of the carbon fibres within the onyx, selected at a same location of the specimen, have changed direction by about 90○ in each of these samples due to the presence of a magnetic field, however such remark observed might be fortuitous due to the fact that the authors could not assure that such direction alteration at an identical position is not due to the change of 3D printing pattern though it was unlikely because of no change in geometry feed to the printing machine (i.e. identical.stl file was produced with and without the magnetic field). This was a very exciting result as it shows that the fibres had changed orientation completely towards alignment with the field, and partially agrees with other literature mentioned earlier about short carbon fibres subjected to a magnetic field [15]. To ensure making reliable remarks, one should equip the machine with in-situ monitoring of the short fibres alignments at such magnification (via either optically, thermally or dielectric measurement). Previously, when applying the magnetic field, the polymer composites were placed in a liquid suspension to help to induce alignment. This was because the level of consolidation within the polymer composite was reduced. This project used a similar concept in that low viscosity would help to induce alignment, however in this case, it was the polymer composite itself that was melted without an external liquid suspension, making this result. Furthermore, the material may not have been completely magnetised, but being able to re-orient the flow of the 3D printing layers is a big initiation step in the right direction [15].

As seen in the figures, carbon fibres' length is approx. 1000-μm length having diameter of 100 μm, which agrees with multiple literature sources [15]. The onyx being viewed was polished, therefore the surface was smooth and even. Initially, the unpolished onyx was examined, and as a result the images were less clear than Fig. 7 (not shown herein). When inspecting the PLA, it was more difficult than the onyx to see the exact direction which the nozzle was printing in. This was down to the uniform structure of repeated lactic units making it difficult to determine the resulting formation. Fig. 8 shows a printed PLA sample of standard precision 0.2 mm with no applied magnetic field. The photographs were taken on a microscope of magnification X500, to see the surface of the printed PLA. Each photograph from A-E shows the direction of printing at a different area of the honeycomb arrangement Sections A and B are similar in that they are seemed to have the most disruption with the printing. Section B presents a relatively smooth surface in comparison to the others, and section C is a smooth sur-

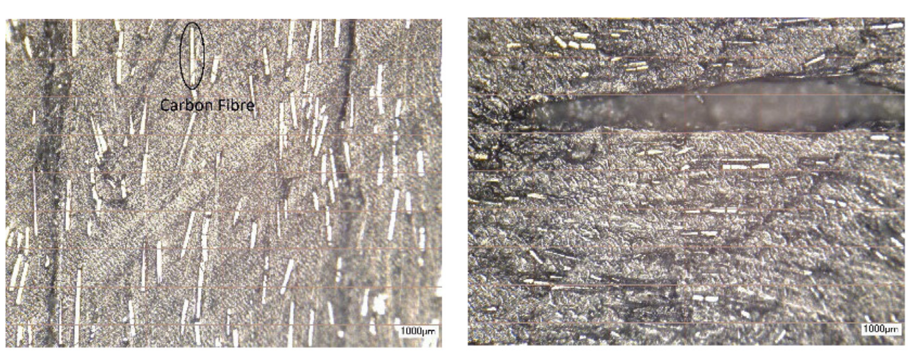


a) Polished onyx with no magnetic field through magnification of X500

b) Polished onyx subjected to two rows of magnets through magnification of X500

**Fig. 7.** Microscopy photos of polished onyx with and without an applied magnetic field (vertical direction is the printing direction).

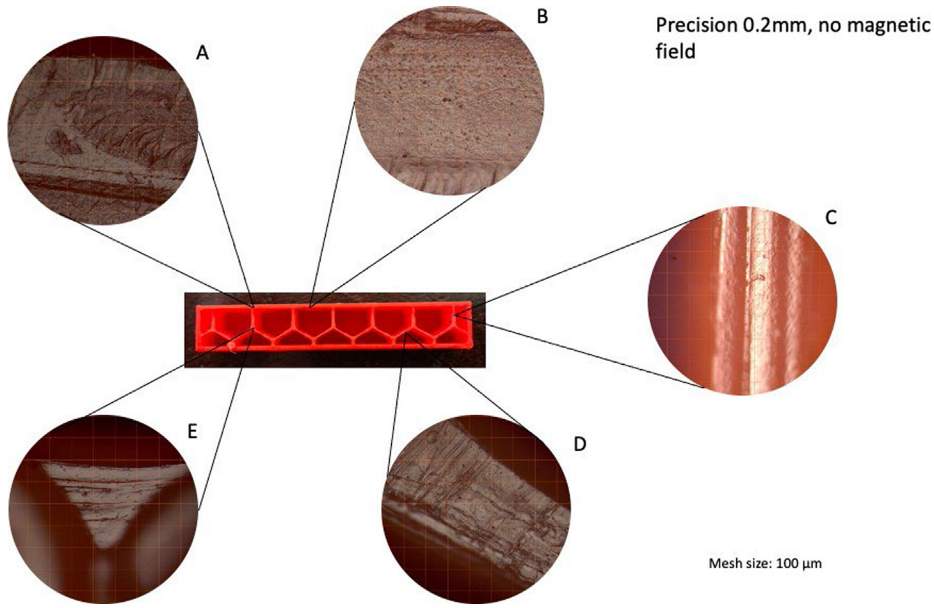


**Fig. 8.** Printed PLA sample with microscopy - A: Side and boundary, B: Side and hole, C: Straight line, D: Tilted line and E: Intersection.

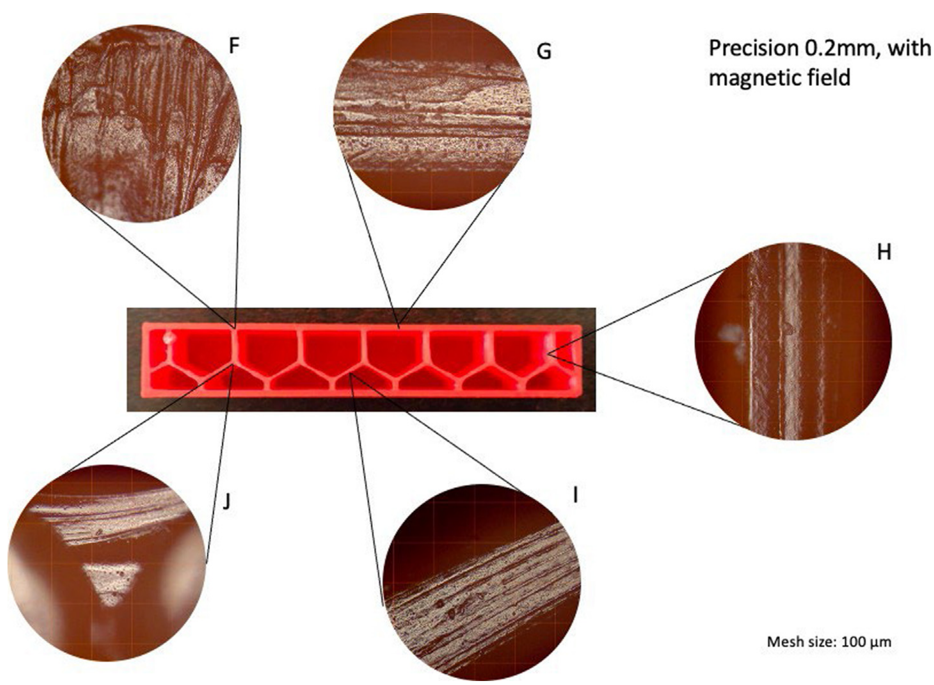


**Fig. 9.** Printed PLA sample with microscopy - F: Side and boundary, G: Side and hole, H: Straight line, I: Tilted line and J: Intersection.

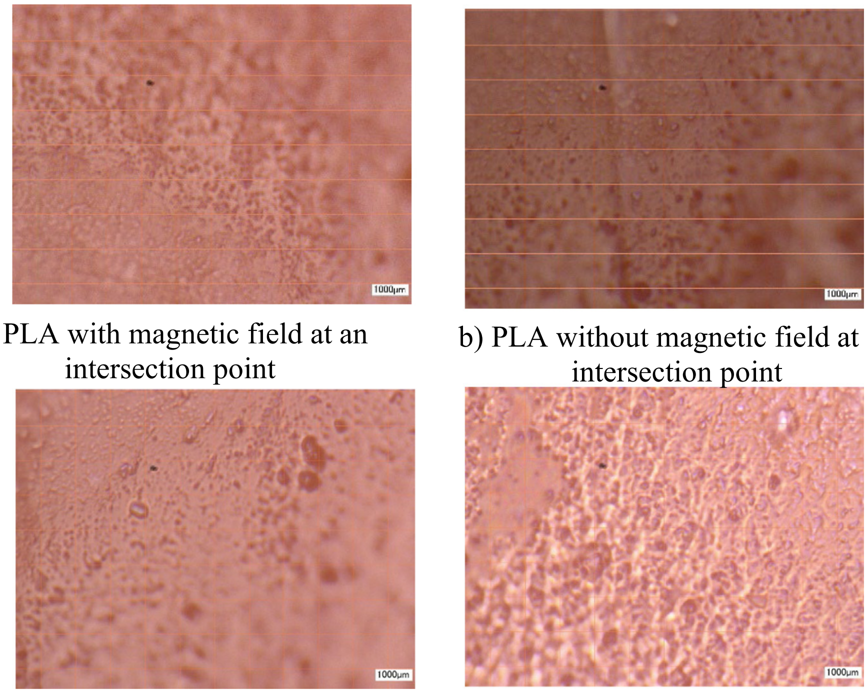

a) PLA with magnetic field at an intersection point

b) PLA without magnetic field at an intersection point

c) PLA with magnetic field at a straight line

d) PLA without magnetic field at a straight line

**Fig. 10.** PLA samples with x5000 magnification.

face with different elevations. Section E only displays a small portion in the centre that is in focus. This is because there is more of an overlap at the intersection where the nozzle is depositing the filament, so this area has varying heights.

Fig. 8 shows a printed PLA sample of standard precision 0.2 mm with two rows of magnets to produce a magnetic field. With this sample, the photograph of every section displays a rough surface, unlike with Fig. 8 where there are a few similarities. It is known that 3D printing using the MakerBot printer cannot be relied on to produce precise duplicates of the same print in terms of the surface texture, despite existing on a flat bed in a flat sample. This is down to the way the molten filament solidifies, as there will be unaccountable irregularities that cannot be controlled, such as air bubbles and uneven temperature control. Therefore, while it is possible that there could be a correlation between the surface consistency and the applied magnetic field, it is very unlikely that this would be visible. So, these differences between Figs. 8 and 9 are better explained by the inconsistent way the molten filament behaves when it solidifies. That being said, these figures show the vertical direction of the printing, which is shown by the line grooves in each photographed section. In this regard, there is reliability between the figures. E and J are the equivalent sections, and they are particularly similar in the direction of the grooves and the focus. This is observed in the images presented in Fig. 10.

The images of X5000 with and without the field can be viewed in Fig. 9. Sections (a), (b), (c) and (d) all look more or less the same as one another, despite being taken from different areas of the sample with and without a magnetic field. Because of this, not much information can be taken for the images at a magnification of x5000, apart from that they all display the rough surface discussed above of dried PLA, presumably from air bubbles or other inconsistencies. Although this magnification is stronger than X500, it still only shows surface of the PLA, so more in the way of fibre alignment could be visible with a stronger magnification.

Though some re-orientations in short fibres are observed in the SEM images from the Onyx samples subjected to in-situ magnetic field, it was difficult to draw any conclusion as to determine whether such re-orientations are the result of 3D printing pattern or magnetic field. typically shown in Fig. 11. The identification of further re-orientation at smaller scale that that in optical microscopy was not possible to achieve during the SEM investigations, meaning that the optical microscopic images were sufficient at the scale this research needed to investigate the alignment possibilities.

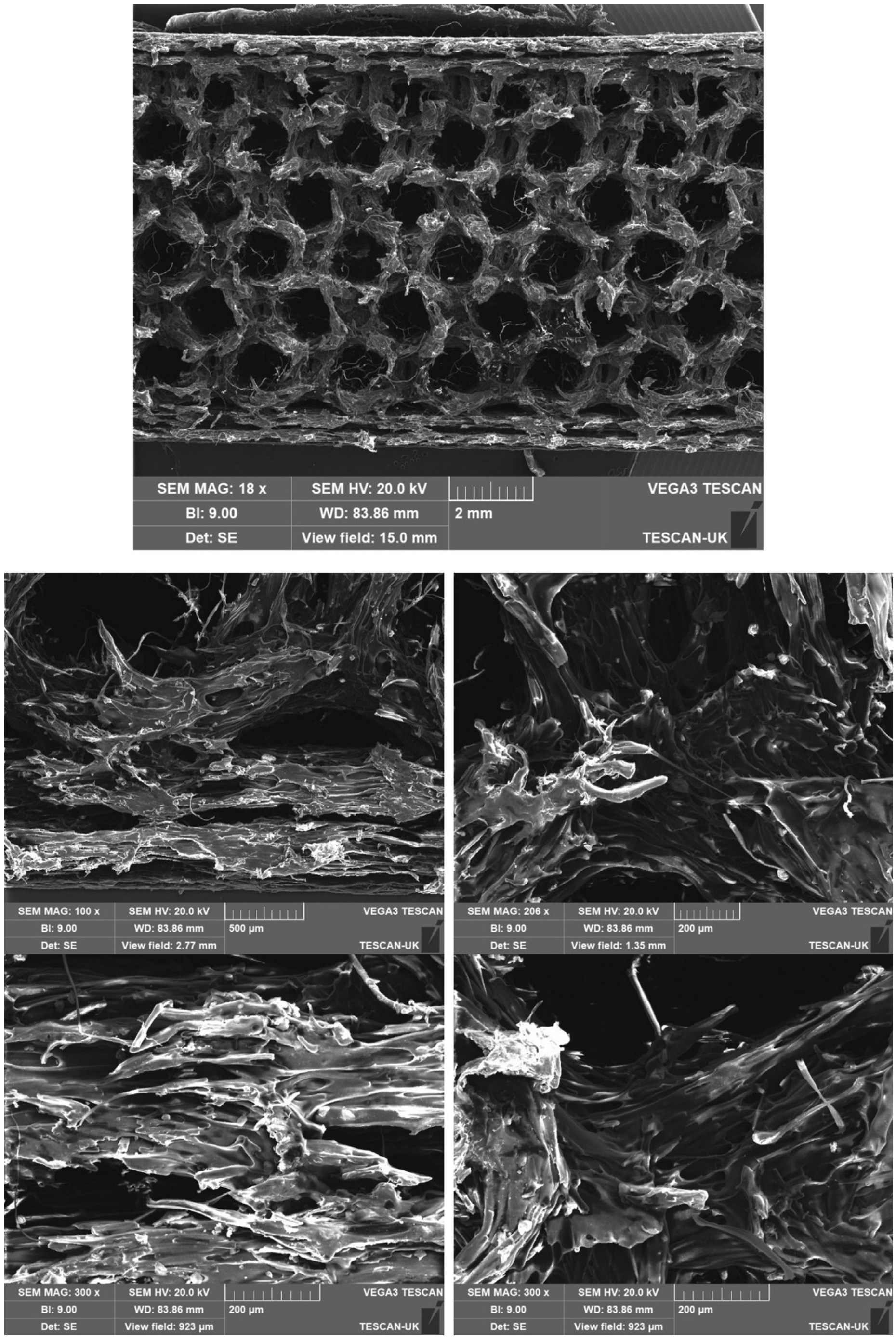


**Fig. 11.** Typical SEM images of carbon composite Onyx subjected to in-situ magnetic field during 3D printing.

## 5. Conclusions

In conclusion, the aim of this project was to see how polymers and short fibre carbon composites react to a relatively strong magnetic field. Though some observations at identical positions 3D printing in carbon composites with and without magnetic field indicated fibres' remote alignment, the results remained fortuitous and qualitative due to the fact that real-time potential alignment was not monitored during the 3D printing, and the disparity between the theory and the observations, i.e. the observations showed much larger re-orientation of short fibres than what predicted by the theory. The PLA and onyx were successfully printed with and without the applied magnetic field and a microscopy of each sample was taken. Onyx showed a significant 90○C change in carbon fiber alignment between the samples with and without the magnetic field, also reported in a number of existing literature. Although a re-alignment seems to have taken place, the material may not have been permanently or temporarily magnetized: The onyx did not appear to have had any change in polarisation. However, perhaps if a stronger magnet or alternating induced fields had been used, a more obvious change would have been detected. Further investigation is needed in terms of equipment of the 3D printing machine with real-time monitoring of possible alignments. A numerical simulation is ongoing for scaling up the theoretical constitutive equations to multiple short fibres scenario at 16% volume fraction (Onyx case) using COMSOL where the 3D printing polymer process parameters will be accounted for.

## Declaration of Competing Interest

The authors declare that they have no known competing financial interests or personal relationships that could have appeared to influence the work reported in this paper.

## Acknowledgement

The author would like to thank Keith Pamment, Richard Leach and Kugathasan Subramaniam for their aid and assistance throughout the technical portion of this project.

## References

[1] F. Ghebretinsae, O. Mikkelsen, A.D. Akessa, Strength analysis of 3D printed carbon fibre reinforced thermoplastic using experimental and numerical methods, IOP Conf. Ser.: Mater. Sci. Eng. 700 (1) (2019) 012024, https://doi.org/10.1088/1757-899X/700/1/012024.

[2] A. Sadeqi, H. Rezaei Nejad, R.E. Owyeung, S. Sonkusale, Three-dimensional printing of metamaterial embedded geometrical optics (MEGO), Microsyst Nanoeng 5 (1) (2019), https://doi.org/10.1038/s41378-019-0053-6.

[3] I. Blanco, The Use of Composite Materials in 3D Printing, J. Compos. Sci. 4 (2) (2020) 42.

[4] A.K. Bastola, M. Hossain, The shape-morphing performance of magnetoactive soft materials, Mater. Des. 211 (2021) 110172, https://doi.org/10.1016/j.matdes.2021.110172.

[5] S. Agarwala, G.L. Goh, G.D. Goh, V. Dikshit, W.Y. Yeong, 3D and 4D printing of polymer/CNTs-based conductive composites, 3D and 4D Printing Polym. Nanocompos. Mater. 10 (2020) 297–324.

[6] M. Naghavi Zadeh, I. Dayyani, M. Yasaee, Fish Cells, a new zero Poisson's ratio metamaterial—Part I: Design and experiment, J. Intell. Mater. Syst. Struct. 31 (13) (2020) 1617–1637.

[7] F. Khan, H. Yazdani Nezhad, 3D Printing of Multi-material Polymer Composite Systems, (2020).

[8] S.C. Daminabo, S. Goel, S.A. Grammatikos, H.Y. Nezhad, V.K. Thakur, Fused deposition modeling-based additive manufacturing (3D printing): techniques for polymer material systems, Mater. Today Chem. 16 (2020) 100248, https://doi.org/10.1016/j.mtchem.2020.100248.

[9] T.P. Hernandez, A.R. Mills, H.Y. Nezhad, Shear Driven Deformation and Damage Mechanisms in High-performance Carbon Fibre-reinforced Thermoplastic and Toughened Thermoset Composites Subjected to High Strain Loading, Compos. Struct. (2020), https://doi.org/10.1016/j.compstruct.2020.113289, 113289–113289.

[10] T. Bregar, D. An, S. Gharavian, M. Burda, I. Durazo-Cardenas, V.K. Thakur, D. Ayre, M. Słoma, M. Hardiman, C. McCarthy, H. Yazdani Nezhad, Carbon nanotube embedded adhesives for real-time monitoring of adhesion failure in high performance adhesively bonded joints, Sci. Rep. 10 (1) (2020), https://doi.org/10.1038/s41598-020-74076-y.

[11] T. Khaleque, X. Zhang, V. Kumar Thakur, I. Aria, H. Yazdani Nezhad, Tailoring of Thermo-Mechanical Properties of Hybrid Composite-Metal Bonded Joints, Polymers 13 (2) (2021) 170, https://doi.org/10.3390/polym13020170.

[12] D. An, J. Nourry, S. Gharavian, V.K. Thakur, I. Aria, I. Cardenas, T. Khaleque, H. Yazdani Nezhad, Strain Self-Sensing Tailoring in Functionalised Carbon Nanotubes/Epoxy Nanocomposites in Response to Electrical Resistance Change Measurement (2020), in: TESConf 2020 - 9th International Conference on Through-life Engineering Services, 2020, https://doi.ogr/10.2139/ssrn.3718026.

[13] K. Tsunehisa, M. Yamato, (2018). (https://www.mdpi.com/journal/polymers/special issues/Magnetic Field Polymer Research).

[14] J. Ciambella, D.C. Stanier, S.S. Rahatekar, Magnetic alignment of short carbon fibres in curing composites, Compos. B Eng. 109 (2017) 129–137.

[15] A. Sierra-Romero, B. Chen, Strategies for the preparation of polymer composites with complex alignment of the dispersed phase, Nanocomposites 4 (4) (2018) 137–155.

[16] M. Pishvar, M. Amirkhosravi, M.C. Altan, Magnet Assisted Composite Manufacturing: A Flexible New Technique for Achieving High Consolidation Pressure in Vacuum Bag/Lay-Up Processes, J. Visualized Exp. (135) (2018), https://doi.org/10.3791/57254.

[17] E. Vitz, J.W. Moore, J. Shorb, X. Prat-Resina, R.E. et al., Cross-Linking. Chemical Education Digital Library (ChemEd DL), 2021. (https://chem.libretexts.org/@go/page/49490).

[18] C. Valdivieso, Magnetic field impacts the fiber alignment of a 3D printed part. 3Dnatives, (2021) (https://www.3dnatives.com/en/magnetic-field-3d-printing-270520204/).

[19] N. Rattanachueskul, A. Saning, S. Kaowphong, N. Chumha, L. Chuenchom, Magnetic carbon composites with a hierarchical structure for adsorption of tetracycline, prepared from sugarcane bagasse via hydrothermal carbonization coupled with simple heat treatment process, Bioresour. Technol. 226 (2017) 164–172.

[20] Technical data sheet PLA. (2019). (https://www.bcn3d.com/wp-content/uploads/2019/09/BCN3D FILAMENTS Technical Data Sheet PLA EN.pdf).

[21] Raman spectroscopy. (2021) Wikipedia. (https://en.wikipedia.org/wiki/Raman spectroscopy).

[22] Technical Specifications. (2021) (https://www.magnet-shop.com/technical-specifications).

[23] T. Kimura, Y. Umehara, F. Kimura, Fabrication of a short carbon fiber/gel composite that responds to a magnetic field, Carbon 48 (2010) 4015–4018.

[24] S.-h. Hwang, S.-K. Lee, Efficient Experimental Design for Measuring Magnetic Susceptibility of Arbitrarily Shaped Materials by MRI, Investig Magn Reson Imaging 22 (3) (2018) 141, https://doi.org/10.13104/imri.2018.22.3.141.